


 Cite this: *Chem. Commun.*, 2020, 56, 1533

 Received 17th September 2019,
 Accepted 23rd December 2019

DOI: 10.1039/c9cc07292f

rsc.li/chemcomm

There is nothing wrong with being soft: using sulfur ligands to increase axially in a Dy(III) single-ion magnet†

 Angelos B. Canaj,^a Sourav Dey,^b Oscar Céspedes,^c Claire Wilson,^a Gopalan Rajaraman^{b*} and Mark Murrie^{b,a}

A new air-stable sulfur-ligated Dy(III) single-ion magnet has been successfully isolated with $U_{\text{eff}} = 638$ K and hysteresis loops open up to 7 K. *In silico* studies show that the S co-ligands significantly boost the axially and that Te- and Se-donors have the potential to further enhance the magnetic properties.

The interest in Single-Molecule Magnets (SMMs), *i.e.* molecular systems, which display the ability to block magnetisation, resulting in the appearance of magnetic hysteresis of molecular origin,¹ is because these systems could revolutionise electron spin-based technologies.² Lanthanide SMMs are often associated with large magnetic moments and large magnetic anisotropy, with Dy(III) being a key component of single-ion magnets (SIMs).³ Through the combination of theory⁴ and experiment, an exciting era has emerged with a new generation of SMMs/SIMs showing impressive energy barriers⁵ and high blocking temperatures, T_B ,⁶ reaching 80 K.⁷ In fact, complexes with D_{3h} ,⁸ D_{4d} ⁹ and D_{5h} ,¹⁰ axial point group symmetries are very promising. Our group recently reported the blueprint for generating strong uniaxial magnetic anisotropy for Dy(III) in $\sim D_{6h}$ symmetry (hexagonal bipyramidal), by combining a strong linear axial ligand field with a weak equatorial ligand field, by using a polydentate ligand L^{N6} ($L^{N6} = N6$ -hexagonal plane from the neutral Schiff base ligand formed from 2,6-diacetylpyridine and ethylenediamine).¹¹

Most of the reported 4f-SIMs incorporate traditional ligands with O-, N-, C- and halogen-donor atoms.³ Rarer are the examples of SMMs exploring ligands with more “exotic” donor atoms from the main group, as was reviewed recently by Guo *et al.*¹² Recently we have explored how ligand electronics can

tune SIM properties¹³ and herein, we sought to explore how different donor groups originating from the p block affect the magnetisation dynamics. We report for the first time the synthesis, structure, magnetic characterisation and *ab initio* studies of $[\text{Dy}^{\text{III}}L^{\text{ON3}}(\text{C}_5\text{H}_{10}\text{NS}_2)_2] \cdot 0.5\text{THF}$ (**1**) (Fig. 1) which is a S-ligated single-ion magnet with hysteresis loops open up to 7 K and a magnetisation reversal barrier of $U_{\text{eff}} = 638$ K, which is unprecedented in the very small family of S-ligated Dy(III) single-ion magnets (see Table 1).^{14–20} Compound **1** was isolated by using the cage-like ligand *N*-(3,5-di-*tert*-butyl-2-hydroxybenzyl)-*N,N*-bis(2-pyridylmethyl)amine (HL^{ON3}) (see ESI†).²¹

Our synthetic strategy generates one short Dy–O bond, to direct the magnetic anisotropy,²² and three longer Dy–N bonds.²³ The rest of the coordination sphere is completed with soft S-donor groups, by using diethyldithiocarbamate co-ligands, (Fig. 1) giving longer Dy–S bonds (Fig. S1 and Table S2, ESI†). Importantly, through a detailed *in silico* study we also examine how O-, Se- and Te-based co-ligands affect the calculated magnetisation reversal barrier, U_{cal} , of **1**.

Complex **1** (Fig. 1) was isolated from a dry THF solution (see ESI†) with the phase purity of the bulk sample confirmed by powder X-ray diffraction (Fig. S2, ESI†). Continuous shape measures²⁴ analysis gives a value of 2.7 for a biaugmented trigonal prism geometry (C_{2v} symmetry) (Fig. S3 and Table S3, ESI†).

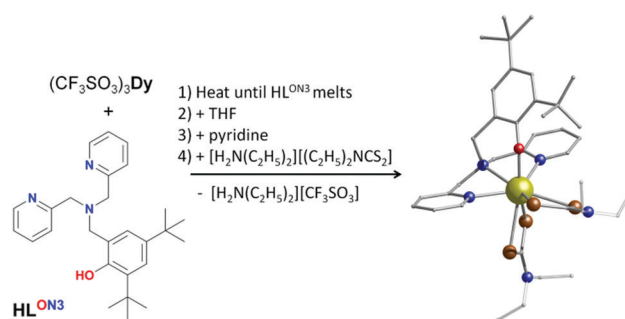


Fig. 1 Synthesis and structure of **1**. Dy, gold; O, red; N, blue; S, brown; C, grey. H atoms and solvent are omitted for clarity.

^a School of Chemistry, University of Glasgow, University Avenue, Glasgow, G12 8QQ, UK. E-mail: mark.murrie@glasgow.ac.uk

^b Department of Chemistry, Indian Institute of Technology Bombay, Powai, Mumbai, Maharashtra, 400076, India. E-mail: rajaraman@chem.iitb.ac.in

^c School of Physics and Astronomy, University of Leeds, Leeds LS2 9JT, UK

† Electronic supplementary information (ESI) available: Experimental section, magnetic studies, crystallographic details, *ab initio* studies. CCDC 1950766. For ESI and crystallographic data in CIF or other electronic format see DOI: 10.1039/c9cc07292f



Table 1 The small family of Dy(III) SIMs/SMMs with S-based ligands

Complex	U_{eff} (K)	τ_0 (s)	H_{dc} (Oe)	Ref.
[Dy ^{III} (Pc)(STBPP)]	194	4.7×10^{-8}	0	14
[(dtc) ₃ Dy(dmbipy)]	9.8	1.9×10^{-6}	1000	15
[(dtc) ₃ Dy(phen)]	20	1.80×10^{-8}	400	16
[(dbm) ₂ Dy(dtc)(phen)]	45	2.8×10^{-8}	1000	16
	40	4.1×10^{-8}	0	
[Dy((-)-pbipy)(pdtc) ₃]	56.7	4.2×10^{-7}	3000	17
Dy ₂ S@C ₈₂ -C _{3v}	6.5	3.6		18
	48	6.2×10^{-4}		
	1232	6.0×10^{-13}		
[Li(thf) ₄][Dy ₄ {N(SiMe ₃) ₂ } ₄ (μ-SEt) ₈ (μ ₄ -SEt)]	66	4.3×10^{-6}	0	19
	71	2.1×10^{-6}	2000	
[(Cp ₂ 'Dy(μ-SSiPh ₃) ₂)]	192	2.38×10^{-7}	0	20
[Dy ^{III} L ^{ONs} (C ₅ H ₁₀ NS ₂) ₂]	638	2.99×10^{-12}	0	This work

The only strong oxygen donor group in **1** has a relatively short Dy–O bond length (2.1591(16) Å) while the Dy–N and Dy–S bonds fall in the range of 2.5237(18)–2.5711(17) Å and 2.8133(5)–2.9647(6) Å, respectively (Table S2 and Fig. S1, ESI†). Additionally, there is no intermolecular hydrogen bonding in **1**, while the shortest Dy···Dy distance is 8.39 Å (Fig. S4, ESI†).

The dc magnetic susceptibility and magnetisation measurements for **1** are shown in Fig. S5 (ESI†). The field cooled (FC) and zero-field cooled (ZFC) magnetic susceptibility show divergence at 5 K (Fig. S6, ESI†) with the magnetic hysteresis measurements, $M(H)$ loops, performed on a powder sample of **1**, remaining open up to 7 K (average sweep rate of 20 mT s⁻¹) (Fig. 2 upper and Fig. S7, ESI†).

Measurements of the variable temperature alternating current (ac) susceptibility between 1–940 Hz were performed in order to investigate the dynamics of the magnetisation for **1** (Fig. 2 lower and Fig. S8–S16, ESI†). Under zero external dc field, the out-of-phase, χ_M'' magnetic susceptibility data exhibit well-defined maxima with χ_M'' peaks clearly observable up to ~35 K (Fig. S8, ESI†), indicating a high magnetisation reversal barrier. The relaxation times, τ , were extracted from the fits of the Argand plots of χ_M'' vs. χ_M' using the generalized Debye model (Fig. S11, ESI†).²⁵ The α parameters found are in the range of 0–0.3 (2–40 K) for **1**. The τ^{-1} vs. T data were fitted using the equation $\tau^{-1} = \tau_{\text{QTM}}^{-1} + CT^n + \tau_0^{-1} \exp(-U_{\text{eff}}/T)$, in which C and n are parameters of the Raman process and τ_{QTM} is the rate of the quantum tunnelling of magnetisation (QTM).²⁶ The best fit gives a magnetisation reversal barrier, U_{eff} of 638 K, $\tau_0 = 2.99 \times 10^{-12}$ s, $n = 3.24$, $C = 0.02 \text{ K}^{-n} \text{ s}^{-1}$, $\tau_{\text{QTM}} = 0.017$ s, under zero dc field (Fig. S17, ESI†) and $U_{\text{eff}} = 656$ K, $\tau_0 = 1.94 \times 10^{-12}$ s, $n = 3.96$ and $C = 3.95 \times 10^{-5} \text{ K}^{-n} \text{ s}^{-1}$ under an optimum field of 1200 Oe (Fig. S18, ESI†). The observed values of the pre-factor τ_0 ,¹⁰ C and n are within the commonly observed range for Dy(III) SMMs.³ The exponent n of the Raman process has a smaller value than expected for a Kramers ion ($n = 9$) suggesting the presence of Raman processes involving optical acoustic phonons.²⁶ To the best of our knowledge, this is the largest magnetisation reversal barrier observed for a Dy(III) single-ion magnet that has S-donor ligands (see Table 1).

In order to gain insight into the mechanism that governs the magnetic relaxation of **1**, we have performed *ab initio* calculations

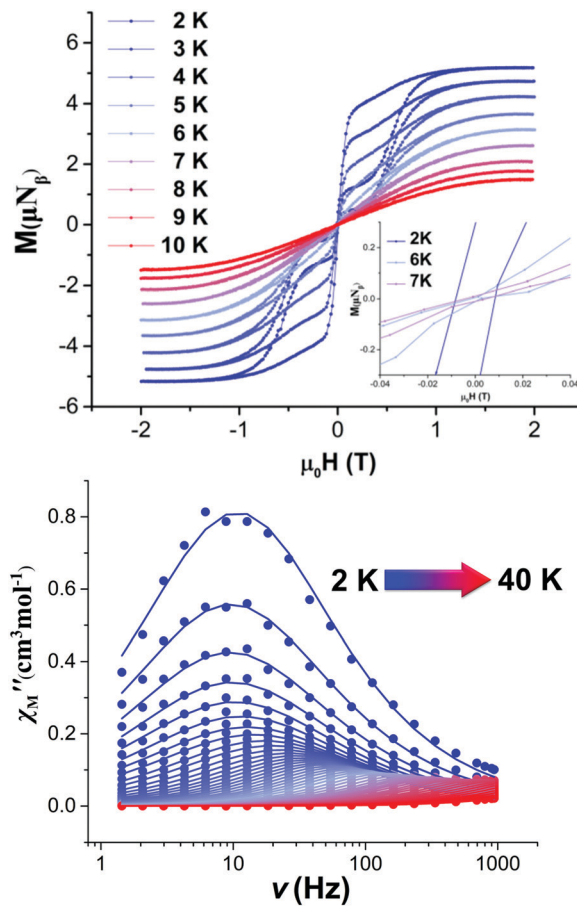


Fig. 2 (upper) Powder magnetic hysteresis measurements for **1** with an average sweep rate of 20 mT s⁻¹. (upper inset) $M(H)$ loops open up to 7 K for **1**. (lower) Plots of $\chi_M''(\nu)$ in zero applied dc field in the temperature range of 2–40 K for **1**.

using the CASSCF/RASSI-SO/SINGLE_ANISO approach implemented in MOLCAS 8.2²⁷ (see ESI†). The eight Kramers Doublets (KDs) in **1** span an energy range of 964 K (Table S4, ESI†). The ground state ($m_J = \pm 15/2$) of the Dy(III) ion in **1** is highly anisotropic with near-perfect axiality ($g_{zz} = 19.859$, $g_{xx} = g_{yy} = 0.001$, Table S4, ESI†). The main anisotropy axis is nearly collinear with the relatively short Dy–O bond (Fig. S19, ESI†) resulting from our synthetic strategy.



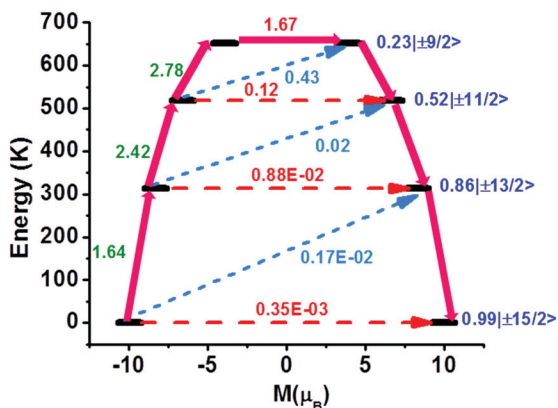


Fig. 3 *Ab initio* calculated relaxation dynamics for **1**. The arrows show the connected energy states with the number representing the matrix element of the transverse moment (see text for details). The black line indicates the KDs as a function of magnetic moments. The red dashed arrow represents QTM (QTM = quantum tunnelling of the magnetisation) *via* the ground state and TA-QTM (TA-QTM = thermally assisted QTM) *via* excited states. The blue dashed arrow indicates possible Orbach processes. The pink thick arrow indicates the mechanism of magnetic relaxation. The numbers above each arrow represent corresponding transverse matrix elements for the transition magnetic moments.²⁹

Using the CASSCF wavefunction, the computed Loprop²⁸ charge on the oxygen atom is found to be nearly three times larger than the nitrogen atoms of the L^{ON3} ligand and twice as large as the sulfur atoms of the diethyldithiocarbamate ligands (Fig. S20, ESI[†]). The axial nature is also observed for the first and second excited states ($m_j = \pm 13/2$, $g_{xx} = 0.023$, $g_{yy} = 0.028$, $g_{zz} = 17.359$ and $m_j = \pm 11/2$, $g_{xx} = 0.281$, $g_{yy} = 0.380$, $g_{zz} = 14.372$, Table S4, ESI[†]), with the higher KDs showing relatively stronger admixtures (Fig. 3). The maximum calculated relaxation barrier, U_{cal} , is estimated at 651 K (Fig. 3), which is in excellent agreement with the experimentally determined magnetisation reversal barrier (U_{eff}) of 638 K found in zero applied dc field. A relatively small transverse magnetic moment is calculated for the first three KDs (0.35×10^{-3} , 0.88×10^{-2} , $1.2 \times 10^{-1} \mu_B$, respectively), which indicates relaxation *via* the third excited state (Fig. 3). In addition, the Orbach processes for the m_j and $m_j + 1$ excited states of opposite magnetisation between the first four KDs are found to be very small ($\leq 0.43 \mu_B$, Fig. 3).

To investigate the importance of the coordination environment and the ligand electronics on the magnetisation dynamics of **1**, we have changed the co-ligand coordination environment *in silico*. We have created a family of three different model systems and used *ab initio* calculations to examine how O-, Te- and Se-based co-ligands affect the calculated magnetisation reversal barrier of **1** (Fig. 4 and Fig. S21, S22, ESI[†]). Importantly, replacing the S-atoms of the diethyldithiocarbamate co-ligands with more commonly used oxygen donors (*i.e.* common carboxylate ligands, model **1-O**, Fig. S22 upper, ESI[†]) gives stronger transverse components, with larger g_{xx}/g_{yy} values obtained for the ground and excited states (see Table S5 (ESI[†]) for model **1-O**). Specifically, the QTM probabilities are calculated to be larger for the first three KDs of model **1-O** (0.63×10^{-3} , 0.31×10^{-1} and $0.85 \mu_B$, see Fig. S21 upper, ESI[†]) compared to **1** (Fig. 3), leading to a smaller calculated barrier of

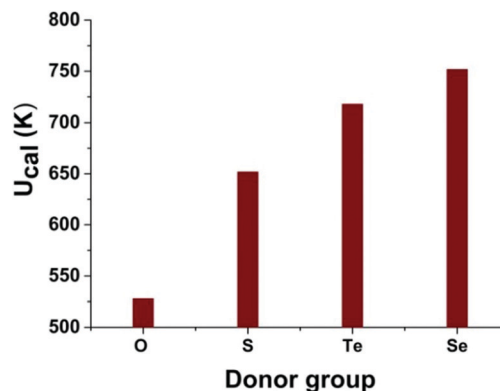


Fig. 4 The effect of the O-, S-, Te- and Se-donor co-ligands on the U_{cal} barrier using *in silico* models based on **1**.

$U_{\text{cal}} = 528$ K (see Fig. 4 and Fig. S21, Table S5, ESI[†]). These results are similar to earlier observations for Dy–O vs. Dy–S substitution¹⁴ suggesting a likely generality of such behaviour in Dy(III) complexes.

In contrast, the g_{xx}/g_{yy} values obtained for model systems **1-Te** and **1-Se**, where the S-atoms in **1** are replaced with Te- and Se-atoms (Fig. S22 lower, ESI[†]), suggest that the magnetisation relaxes *via* the fourth KD, giving higher calculated barriers of $U_{\text{cal}} = 718$ K for **1-Te** and 752 K for **1-Se** (see Fig. 4 and Fig. S21, Table S5, ESI[†]). Importantly, our results suggest that substitution of the S-atoms in **1** with O-atoms favours a stronger transverse anisotropy, while substitution with Te- and/or Se-atoms stabilises stronger axiality, with smaller transverse magnetic moments calculated for the first four KDs and smaller g_{xx}/g_{yy} values (see Fig. 4 and Fig. S21, Table S5, ESI[†]). This is in excellent agreement with a study performed on pnictogen-ligated compounds.³⁰ The ratio between B_2^0 and the corresponding non-axial crystal field parameters increases in the following order **1-O** < **1** < **1-Te** < **1-Se** (Table S7, ESI[†]) in line with the increasing U_{cal} barrier (Fig. 4).

In conclusion, $[\text{Dy}^{\text{III}}\text{L}^{\text{ON3}}(\text{C}_5\text{H}_{10}\text{NS}_2)_2] \cdot 0.5\text{THF}$ (**1**) is the first S-ligated single-ion magnet with hysteresis loops open up to 7 K and a magnetisation reversal barrier of 638 K, which is significantly higher than any reported Dy(III) SIM that has S-donor ligands (Table 1). This novel complex was isolated by a carefully designed synthetic strategy that generates one short Dy–O bond,²² which directs the magnetic anisotropy, combined with three longer Dy–N bonds, with the remainder of the coordination sphere completed with soft S-donor groups, giving longer Dy–S bonds. Furthermore, through detailed *in silico* studies we examine how O-, Se- and Te-based co-ligands affect the calculated magnetisation reversal barrier and magnetisation dynamics in **1**, finding higher U_{cal} values for Te- and Se-based co-ligands. We hope that this study will generate further interest in the investigation of S-ligated SIMs and prompt the study of new Te- and Se-ligated SIMs.

We thank EPSRC UK (EP/N01331X/1, EP/M000923/1); UGC (SRF fellowship); UGC-UKIERI (184-1/2018(IC)); UGC and SERB (CRG/2018/000430); CSIR (01(2980)/19/EMR-II) and IIT Bombay (CRAY supercomputing facility) for funding.



Conflicts of interest

There are no conflicts to declare.

Notes and references

- 1 S. M. J. Aubin, M. W. Wemple, D. M. Adams, H.-L. Tsai, G. Christou and D. N. Hendrickson, *J. Am. Chem. Soc.*, 1996, **118**, 7746; R. Sessoli, H. L. Tsai, A. R. Schake, S. Wang, J. B. Vincent, K. Folting, D. Gatteschi, G. Christou and D. N. Hendrickson, *J. Am. Chem. Soc.*, 1993, **115**, 1804; A. Caneschi, D. Gatteschi, R. Sessoli and M. A. Novak, *Nature*, 1993, **365**, 141; C. J. Milios, A. Vinslava, W. Wernsdorfer, S. Moggach, S. Parsons, S. P. Perlepes, G. Christou and E. K. Brechin, *J. Am. Chem. Soc.*, 2007, **129**, 2754.
- 2 E. M. Pineda, C. Godfrin, F. Balestro, W. Wernsdorfer and M. Ruben, *Chem. Soc. Rev.*, 2018, **47**, 501; R. Vincent, S. Klyatskaya, M. Ruben, W. Wernsdorfer and F. Balestro, *Nature*, 2012, **488**, 357; M. Shiddiq, D. Komijani, Y. Duan, A. Gaita-Ariño, E. Coronado and S. Hill, *Nature*, 2016, **531**, 348; C. Godfrin, A. Ferhat, R. Ballou, S. Klyatskaya, M. Ruben, W. Wernsdorfer and F. Balestro, *Phys. Rev. Lett.*, 2017, **119**, 187702; A. Gaita-Ariño, F. Luis, S. Hill and E. Coronado, *Nat. Chem.*, 2019, **11**, 301; M. Atzori and R. Sessoli, *J. Am. Chem. Soc.*, 2019, **141**, 11339.
- 3 M. Heras Ojea, L. H. C. Maddock and R. A. Layfield, Lanthanide Organometallics as Single-Molecule Magnets, in *Topics in Organometallic Chemistry*, Springer, Berlin, Heidelberg, 2019; F.-S. Guo and R. A. Layfield, *Acc. Chem. Res.*, 2018, **51**, 1880; M. Feng and M.-L. Tong, *Chem. – Eur. J.*, 2018, **24**, 7574; A. K. Bar, P. Kalita, M. K. Singh, G. Rajaraman and V. Chandrasekhar, *Coord. Chem. Rev.*, 2018, **367**, 163; S. G. McAdams, A.-M. Ariciu, A. K. Kostopoulos, J. P. S. Walsh and F. Tuna, *Coord. Chem. Rev.*, 2017, **346**, 216; Z. Zhu, M. Guo, X.-L. Li and J. Tang, *Coord. Chem. Rev.*, 2019, **378**, 350; L. Spree and A. A. Popov, *Dalton Trans.*, 2019, **48**, 2861.
- 4 L. Ungur and L. F. Chibotaru, *Inorg. Chem.*, 2016, **55**, 10043; J. D. Rinehart and J. R. Long, *Chem. Sci.*, 2011, **2**, 2078; N. F. Chilton, *Inorg. Chem.*, 2015, **54**, 2097; A. Lunghi, F. Totti, R. Sessoli and S. Sanvito, *Nat. Commun.*, 2017, **8**, 14620.
- 5 S.-D. Jiang, B.-W. Wang, H.-L. Sun, Z.-M. Wang and S. Gao, *J. Am. Chem. Soc.*, 2011, **133**, 4730; Y.-S. Meng, L. Xu, J. Xiong, Q. Yuan, T. Liu, B.-W. Wang and S. Gao, *Angew. Chem., Int. Ed.*, 2018, **57**, 1; Y.-S. Ding, K.-X. Yu, D. Reta, F. Ortu, R. E. P. Winpenny, Y.-Z. Zheng and N. F. Chilton, *Nat. Commun.*, 2018, **9**, 3134; S. Demir, M. I. Gonzalez, L. E. Darago, W. J. Evans and J. R. Long, *Nat. Commun.*, 2017, **8**, 2144; P. E. Kazin, M. A. Zykina, V. V. Utochnikova, O. V. Magdysyuk, A. V. Vasiliev, Y. V. Zubavichus, W. Schnelle, C. Felser and M. Jansen, *Angew. Chem., Int. Ed.*, 2017, **56**, 1; F. Liu, D. S. Krylov, L. Spree, S. M. Avdoshenko, N. A. Samoylova, M. Rosenkranz, A. Kostanyan, T. Greber, A. U. B. Wolter, B. Buchner and A. A. Popov, *Nat. Commun.*, 2017, **8**, 16098.
- 6 F.-S. Guo, B. M. Day, Y.-C. Chen, M.-L. Tong, A. Mansikkamäki and R. A. Layfield, *Angew. Chem., Int. Ed.*, 2017, **56**, 11445; A. P. Goodwin, F. Ortu, D. Reta, N. F. Chilton and D. P. Mills, *Nature*, 2017, **548**, 439; K. R. McClain, C. A. Gould, K. Chakarawet, S. J. Teat, T. J. Groshens, J. R. Long and B. G. Harvey, *Chem. Sci.*, 2018, **9**, 8492.
- 7 F.-S. Guo, B. M. Day, Y.-C. Chen, M.-L. Tong, A. Mansikkamäki and R. A. Layfield, *Science*, 2018, **362**, 1400.
- 8 P. Zhang, L. Zhang, C. Wang, S. Xue, S.-Y. Lin and J. Tang, *J. Am. Chem. Soc.*, 2014, **136**, 4484; K. L. M. Harriman, J. L. Brosmer, L. Ungur, P. L. Diaconescu and M. Murugesu, *J. Am. Chem. Soc.*, 2017, **139**, 1420.
- 9 J. Wu, J. Jung, P. Zhang, H. Zhang, J. Tang and B. Le Guennic, *Chem. Sci.*, 2016, **7**, 3632; K. Katoh, S. Yamashita, N. Yasuda, Y. Kitagawa, B. K. Breedlove, Y. Nakazawa and M. Yamashita, *Angew. Chem., Int. Ed.*, 2018, **57**, 9262; S. Bala, G.-Z. Huang, Z.-Y. Ruan, S.-G. Wu, Y. Liu, L.-F. Wang, J.-L. Liu and M.-L. Tong, *Chem. Commun.*, 2019, **55**, 9939.
- 10 Y.-C. Chen, J.-L. Liu, L. Ungur, J. Liu, Q.-W. Li, L.-F. Wang, Z.-P. Ni, L. F. Chibotaru, X.-M. Chen and M.-L. Tong, *J. Am. Chem. Soc.*, 2016, **138**, 2829; Y.-S. Ding, N. F. Chilton, R. E. P. Winpenny and Y.-Z. Zheng, *Angew. Chem., Int. Ed.*, 2016, **55**, 16071; J. Liu, Y.-C. Chen, J.-L. Liu, V. Vieru, L. Ungur, J.-H. Jia, L. F. Chibotaru, Y. Lan, W. Wernsdorfer, S. Gao, X.-M. Chen and M.-L. Tong, *J. Am. Chem. Soc.*, 2016, **138**, 5441; S. K. Gupta, T. Rajeshkumar, G. Rajaraman and R. Murugavel, *Chem. Sci.*, 2016, **7**, 5181; J. L. Liu, Y. C. Chen, Y. Z. Zheng, W. Q. Lin, L. Ungur, W. Wernsdorfer, L. F. Chibotaru and M. L. Tong, *Chem. Sci.*, 2013, **4**, 3310; A. B. Canaj, M. K. Singh, C. Wilson, G. Rajaraman and M. Murrie, *Chem. Commun.*, 2018, **54**, 8273.
- 11 A. B. Canaj, S. Dey, E. R. Marti, C. Wilson, G. Rajaraman and M. Murrie, *Angew. Chem., Int. Ed.*, 2019, **58**, 14146; A. B. Canaj, S. Dey, E. R. Marti, C. Wilson, G. Rajaraman and M. Murrie, *Angew. Chem.*, 2019, **131**, 14284.
- 12 F.-S. Guo, A. K. Bar and R. A. Layfield, *Chem. Rev.*, 2019, **119**, 8479.
- 13 A. B. Canaj, M. K. Singh, E. R. Marti, M. Damjanović, C. Wilson, O. Céspedes, W. Wernsdorfer, G. Rajaraman and M. Murrie, *Chem. Commun.*, 2019, **55**, 5950.
- 14 W. Cao, C. Gao, Y.-Q. Zhang, D. Qi, T. Liu, K. Wang, C. Duan, S. Gao and J. Jiang, *Chem. Sci.*, 2015, **6**, 5947.
- 15 S.-S. Liu, J.-M. Zhao, S. Deng, J. Xiong, M.-F. Yang, J.-X. Li, S.-J. Lin, Y.-Q. Zhang and B.-W. Wang, *Inorg. Chem. Commun.*, 2018, **95**, 82.
- 16 S.-S. Liu, K. Lang, Y.-Q. Zhang, Q. Yang, B.-W. Wang and S. Gao, *Dalton Trans.*, 2016, **45**, 8149.
- 17 H.-R. Wen, K. Yang, S.-J. Liu, F.-Y. Liang, X.-R. Xie, C.-M. Liu and Y.-W. Li, *Inorg. Chim. Acta*, 2018, **473**, 145.
- 18 C.-H. Chen, D. S. Krylov, S. M. Avdoshenko, F. Liu, L. Spree, R. Yadav, A. Alvertis, L. Hozoi, K. Nenkov, A. Kostanyan, T. Greber, A. Wolter-Giraud and A. A. Popov, *Chem. Sci.*, 2017, **8**, 6451.
- 19 D. N. Woodruff, F. Tuna, M. Bodensteiner, R. E. P. Winpenny and R. A. Layfield, *Organometallics*, 2013, **32**, 1224.
- 20 F. Tuna, C. A. Smith, M. Bodensteiner, L. Ungur, L. F. Chibotaru, E. J. L. McInnes, R. E. P. Winpenny, D. Collison and R. A. Layfield, *Angew. Chem., Int. Ed.*, 2012, **51**, 6976.
- 21 S. Zheng, T. C. Berto, E. W. Dahl, M. B. Hoffman, A. L. Speelman and N. Lehnert, *J. Am. Chem. Soc.*, 2013, **135**, 4902.
- 22 L. Ungur and L. F. Chibotaru, *Phys. Chem. Chem. Phys.*, 2011, **13**, 20086.
- 23 S. K. Singh, T. Gupta and G. Rajaraman, *Inorg. Chem.*, 2014, **53**, 10835.
- 24 M. Pinskya and D. Avnir, *Inorg. Chem.*, 1998, **37**, 5575; D. Casanova, M. Llunell, P. Alemany and S. Alvarez, *Chem. – Eur. J.*, 2005, **11**, 1479.
- 25 D. Gatteschi, R. Sessoli and J. Villain, *Molecular Nanomagnets*, Oxford Univ. Press, Yton, 2006.
- 26 K. N. Shrivastava, *Phys. Status Solidi B*, 1983, **117**, 437; S. Q. Wu, Y. Miyazaki, M. Nakano, S. Q. Su, Z. S. Yao, H. Z. Kou and O. Sato, *Chem. – Eur. J.*, 2017, **23**, 10028; A. Singh and K. N. Shrivastava, *Phys. Status Solidi B*, 1979, **95**, 273.
- 27 F. Aquilante, J. Autschbach, R. K. Carlson, L. F. Chibotaru, M. G. Delcey, L. De Vico, I. Fdez Galvan, N. Ferre, L. M. Frutos and L. Agliardi, *et al.*, *J. Comput. Chem.*, 2016, **37**, 506; L. F. Chibotaru and L. Ungur, *J. Chem. Phys.*, 2012, **137**, 064112; A. A. Granovsky, *J. Chem. Phys.*, 2011, **134**, 214113.
- 28 L. Agliardi, R. Lindh and G. Karlstrom, *J. Chem. Phys.*, 2004, **121**, 4494.
- 29 L. Ungur, M. Thewissen, J. P. Costes, W. Wernsdorfer and L. F. Chibotaru, *Inorg. Chem.*, 2013, **52**, 6328.
- 30 T. Pugh, F. Tuna, L. Ungur, D. Collison, E. J. L. McInnes, L. F. Chibotaru and R. A. Layfield, *Nat. Commun.*, 2015, **6**, 7492; T. Pugh, V. Vieru, L. F. Chibotaru and R. A. Layfield, *Chem. Sci.*, 2016, **7**, 2128.

